JPE 14-5-24

http://dx.doi.org/10.6113/JPE.2014.14.5.1038
ISSN(Print): 1598-2092 / ISSN(Online): 2093-4718

State-of-charge Estimation for Lithium-ion Batteries Using a Multi-state Closed-loop Observer

Yulan Zhao*, Haitao Yun†, Shude Liu*, Huirong Jiao*, and Chengzhen Wang*

*†School of Automobile and Traffic, Qingdao Technological University, Qingdao, China

Abstract

Lithium-ion batteries are widely used in hybrid and pure electric vehicles. State-of-charge (SOC) estimation is a fundamental issue in vehicle power train control and battery management systems. This study proposes a novel model-based SOC estimation method that applies closed-loop state observer theory and a comprehensive battery model. The state-space model of lithium-ion battery is developed based on a three-order resistor–capacitor equivalent circuit model. The least square algorithm is used to identify model parameters. A multi-state closed-loop state observer is designed to predict the open-circuit voltage (OCV) of a battery based on the battery state-space model. Battery SOC can then be estimated based on the corresponding relationship between battery OCV and SOC. Finally, practical driving tests that use two types of typical driving cycle are performed to verify the proposed SOC estimation method. Test results prove that the proposed estimation method is reasonably accurate and exhibits accuracy in estimating SOC within 2% under different driving cycles.

Key words: Closed-loop observer, Electric vehicle, Lithium-ion battery, SOC estimation

I. INTRODUCTION

Lithium-ion battery is a promising power source for hybrid and pure electric vehicles because of its high energy and power density. Accurate state-of-charge (SOC) estimation is important in vehicle power train control and battery management systems [1].

Although the traditional coulomb counting method can realize online SOC measurement, it easily accumulates errors because of incorrect measurements. Moreover, the initial integral value is difficult to measure by using this method. Thus, this method is seldom used alone. Many recent studies have focused on SOC estimation. Methods for SOC estimation generally include voltage-based correction [2], [3], fuzzy logic-based [4]-[8], neural network [9]-[11], and Kalman filter [12]-[21] methods. Wei et al. [2] proposed a method based on current time window to estimate battery SOC of fuel cells for hybrid electric cars. Leksono et al. [3] proposed a coulomb counting method with modified Peukert for SOC estimation on a LiFePO4 battery. The voltage-based correction method periodically revised SOC estimation by battery voltage. The drawback of this method is that its revision is discontinuous and effects on the stability of power system control is easily produced. The main disadvantage of the fuzzy and neural network methods is the unclear physical definition of the model. Moreover, these methods require a huge amount of training data and a suitable training algorithm. Many recent studies have focused on Kalman filter-based methods. Vasebi et al. [12], Hua et al. [13], Jiang et al. [14], Zhou et al. [15], and Piao et al. [16] used the extended Kalman filter in their methods. Santhanagopalan et al. [17], Zhang et al. [18], and He et al. [19] used the unscented Kalman filter in their methods. Choa et al. [20], Xiong et al. [21], and Sepasia et al. [22] adopted an adaptive Kalman filter in their methods. The Kalman filter method is a model-based estimation technique. Most studies on battery SOC estimation in the past five years are related to the Kalman filter method. This method, which is based on the corresponding relationship between SOC and open-circuit voltage (OCV), can realize real-time SOC correction. In practical applications, however, system noises and measurement errors are typically difficult to figure out.

To solve the aforementioned problems in the existing

Manuscript received Apr. 10, 2014; revised Jun. 26, 2014
Recommended for publication by Associate Editor Woo-Jin Choi.
†Corresponding Author: yunht@163.com
Tel: +86-13465811386, Fax: +86-532-86875211, Qingdao Tech. Univ.
*School of Automobile and Traffic, Qingdao Technological University, China

estimation method, we propose a novel model-based battery SOC estimation method that applies closed-loop state observer theory. The proposed estimation method uses a closed-loop feedback algorithm to estimate battery SOC in real time. The influence of system noises and measurement errors can be reduced by feeding back battery voltage. This method presents a clear physical definition and is easily applied in practical control systems. In addition, we present several typical driving cycle tests to prove that the proposed SOC estimation method can solve the problem on initial battery SOC being too difficult to specify in practical applications.

II. STATE-SPACE MODEL OF THE BATTERY

The battery used in this study is lithium iron phosphate with a capacity of 20 Ah. Given the complexity of the internal physical and chemical processes, an accurate physical model of lithium-ion battery is difficult to generate, which is unnecessary for control design. The equivalent circuit model method is widely employed in battery simulation. Thus, this method is adopted in the current study to model lithium-ion battery. The least square identification method is used to calculate model parameters. A three-order resistor–capacitor (RC) equivalent circuit model (Fig. 1) is used to simulate battery behavior. This model was developed based on the FreedomCar battery model of the Partnership for a New Generation of Vehicles, which is a cooperative research project between the United States government and the auto industry. Theory analyses and experiments were conducted in [2] to prove that the three-order RC model exhibits higher accuracy in simulating lithium-ion battery than the FreedomCar model.

In Fig. 1, R0 denotes ohm resistance; R1 and R2 indicate polarized resistance; C0, C1, and C2 are the equivalent capacitors; U_{bus} is the terminal voltage; U_0 is the equivalent OCV of the battery (that is, $U_{bus} = U_0$ after resting for over 3 h); U_1 is the terminal voltage of C1; and U_2 is the terminal voltage of C2.

According to the equivalent circuit model shown in Fig. 1, the following equations can be derived:

$$\begin{cases} C_1 \times \dot{U}_1(t) + U_1(t)/R_1 = -I_b(t) \\ C_2 \times \dot{U}_2(t) + U_2(t)/R_2 = -I_b(t) \\ C_0 \times \dot{U}_0(t) = -I_b \\ U_{bus}(t) = U_0 + U_1 + U_2 - R_0 \times Ib(t) \end{cases}, \quad (1)$$

where I_b is the battery current; C_0, C_1, and C_2 are the capacitance values of C0, C1, and C2, respectively; R_0, R_1, and R_2 are the resistance values of R0, R1, and R2, respectively; and U_0, U_1, and U_2 are the terminal voltages of C0, C1, and C2, respectively.

According to the first three formulas in Eq. (1), the relationship between U_0 and I_b can be expressed as follows:

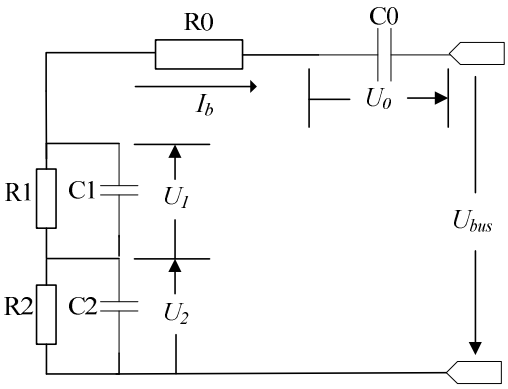

Fig. 1. Equivalent circuit model of lithium-ion battery.

$$U_0(t) = \frac{1}{C_0}\int_0^t [-I_b(t)]dt + U_{0\_init}, \quad (2)$$

where U_{0_init} is the initial value of U_0. U_0 is the terminal voltage of C0. Depending on the equivalent circuit model of the battery, U_0 is also equal to the corresponding OCV of the battery.

The first three formulas in Eq. (1) can be Laplace transformed into transfer functions as follows:

$$\begin{cases} G_{Kb0} = \dfrac{U_0(s)}{I_b(s)} = -\dfrac{1}{C_0 s} \\ G_{Kb1} = \dfrac{U_1(s)}{I_b(s)} = -\dfrac{R_1}{R_1 C_1 s + 1} \\ G_{Kb2} = \dfrac{U_2(s)}{I_b(s)} = -\dfrac{R_2}{R_2 C_2 s + 1} \end{cases}. \quad (3)$$

If we define state vector $x_b = [U_0 \quad U_1 \quad U_2]^T$, input vector $u_b = [I_b]$, and output vector $y_b = [U_{bus}]$, then the state-space equation of the battery mathematical model can be obtained as follows:

$$\begin{cases} \dot{x}_b = Ax_b + Bu_b \\ y_b = Cx_b + Du_b \end{cases}. \quad (4)$$

In Eq. (4),

$$A = \begin{bmatrix} 0 & 0 & 0 \\ 0 & -1/R_1C_1 & 0 \\ 0 & 0 & -1/R_2C_2 \end{bmatrix},$$

$$B = \begin{bmatrix} -1/C_0 \\ -1/C_1 \\ -1/C_2 \end{bmatrix},$$

$$C = \begin{bmatrix} 1 \\ 1 \\ 1 \end{bmatrix}^T, \quad (5)$$

$$D = [-R_0].$$

Eqs. (4) and (5) can be expressed as follows:

$$\begin{cases} \begin{bmatrix} \dot{U}_0 \\ \dot{U}_1 \\ \dot{U}_2 \end{bmatrix} = \begin{bmatrix} 0 & 0 & 0 \\ 0 & -1/R_1C_1 & 0 \\ 0 & 0 & -1/R_2C_2 \end{bmatrix} \begin{bmatrix} U_0 \\ U_1 \\ U_2 \end{bmatrix} + \begin{bmatrix} -1/C_0 \\ -1/C_1 \\ -1/C_2 \end{bmatrix} [I_b] \\ [U_{bus}] = [1 \quad 1 \quad 1] \begin{bmatrix} U_0 \\ U_1 \\ U_2 \end{bmatrix} + [-R_0][I_b] \end{cases} \quad (6)$$

III. Parameter Estimation of the Battery State-Space Model

We use the least square identification method to estimate the parameters of the battery state-space model, namely C_0, C_1, C_2, R_0, R_1, and R_2 in Eq. (6). By using the parameter estimation toolbox of MATLAB software, parameter estimation can be easily conducted in a computer. The test data for battery voltage and current are introduced as sample data to start parameter estimation. Data are gathered from a practical vehicle driving test using a hybrid electric vehicle equipped with a lithium-ion battery pack. A CAN-bus development tool called CANape (Vector Informatik, Stuttgart, Germany) is used in the test to acquire data and calibrate the control parameters. The sample data used in parameter estimation are shown in Figs. 2 and 3. Given that we use the test data from the practical vehicle driving test as sample data for parameter estimation, the estimated results are applicable in practice.

A comparison between the model simulation and the test is conducted and illustrated in Figs. 4 and 5 to verify the performance of the battery state-space model and the parameter estimation results. The test data for battery current and initial OCV are inputted into the battery model during the simulation. The battery voltages in the simulation and test are compared. First, we compare the results of the battery model simulation and battery pulse discharge test (Fig. 4). The discharge current is 60 A, the discharge time is 20 s, and the recovery time is approximately 60 s in the pulse discharge test. Fig. 4 shows that the average error of the simulation is lower than 0.1 V, its maximum error is lower than 0.5 V, and the average margin of the simulation error is lower than 0.2%. Second, we compare the results of the simulation and practical vehicle driving test (Fig. 5). The average error of the simulation is lower than 0.65 V, its maximum error is lower than 5 V, and the average margin of the simulation error is lower than 1.5%. The comparison between the results of the model simulations and the tests proves that the three-order battery model exhibits good accuracy. Although this model offers degrees of freedom in a nonlinear characteristic, immunity from noise and interference during SOC estimation remains a problem. Thus, we propose a multi-state closed-loop method to reduce the influence of noise and interference during SOC estimation. This method is discussed in the next section.

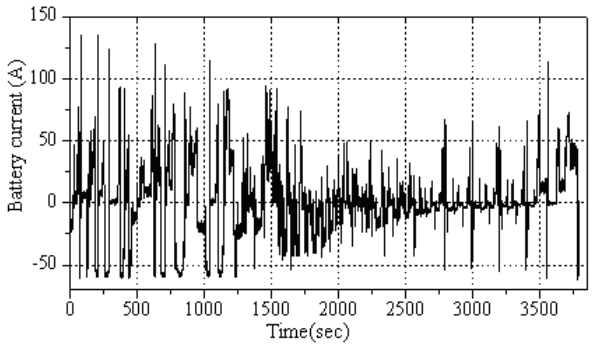

Fig. 2. Test results for battery current in the 1 h driving test.

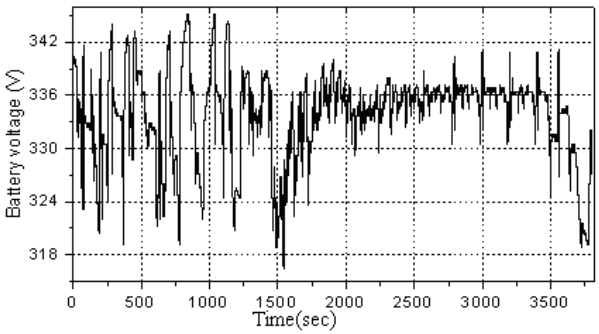

Fig. 3. Test results for battery voltage in the 1h vehicle driving test.

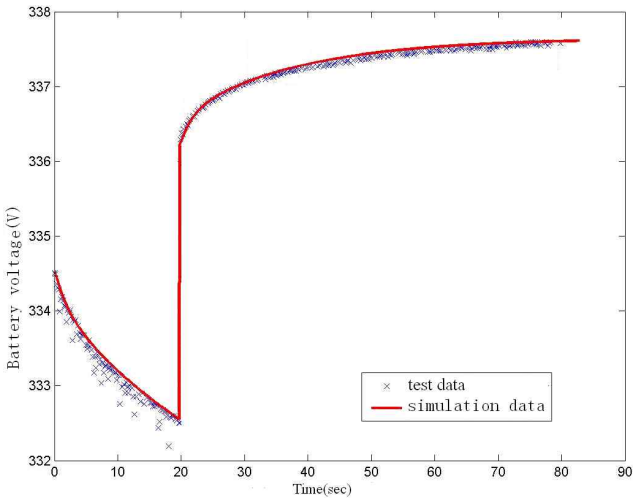

Fig. 4. Comparison between the results of the simulation and the pulse discharge test.

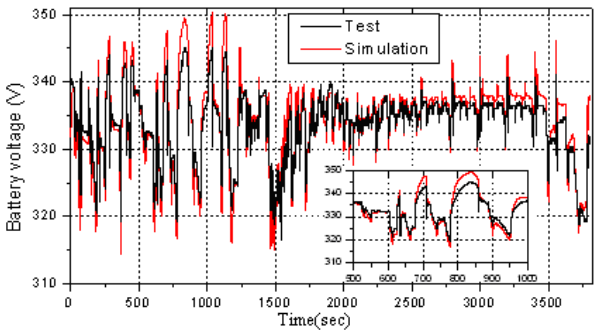

Fig. 5. Comparison between the results of the simulation and the practical vehicle driving test.

IV. BATTERY SOC ESTIMATION

A. Designing the Multi-State Closed-Loop Observer

Fig. 6 shows the relationship between the OCV and SOC of lithium-ion battery, which is obtained by using the battery test bench in [2]. Several single cells are selected from the battery pack as test objects in the test. Fig. 6 shows that when the battery works within the SOC range of 10% to 90% (the general operating range of a battery for vehicle application), a nonlinear corresponding relationship exists between battery OCV and SOC. This relationship is consistent for different single cells of the battery. In addition, the tested single cells are selected randomly and used for different lengths of time. Therefore, we can estimate battery OCV based initially on the battery mathematical model. Battery SOC can be consequently obtained from the corresponding relationship of OCV and SOC. In actual operation, however, estimation accuracy is affected by modeling errors, measuring errors, and random interferences. A closed-loop state observer is designed to solve this problem. This observer is based on the developed state-space model of lithium-ion battery that can eliminate the effects of errors and interferences by feeding back the model estimation error. Thus, this SOC estimation method is theoretically reasonable and feasible.

Fig. 7 shows the schematic of the developed battery state-space model. Fig. 8 shows the schematic of the closed-loop state observer designed in this study. Figs. 7 and 8 shows that $\sum_0$ is used to represent the studied battery. A, B, C, and D are the state matrices defined in Eq. (5). G is the gain matrix of the state observer. The battery state-space model calculates battery state and output through an open-loop technique as shown in Fig. 7. The closed-loop state observer estimates battery state and output via a closed-loop technique as shown in Fig. 8. When the states calculated by the battery model are unequal to real battery states, a deviation exists between battery model output (namely, the estimated battery voltage) and real battery voltage. The state observer feeds back this deviation to the battery model with gain matrix G to correct the estimated state vector $\hat{x}$. With a moderate gain matrix G, the correction can make the estimated states approach the actual states of the battery with moderate speed and reasonable accuracy.

The state equation of the closed-loop state observer is expressed as follows based on Fig. 8:

$$\begin{aligned}\dot{\hat{x}} &= A\hat{x} + Bu + G(y-\hat{y}) \\ &= A\hat{x} + Bu + Gy - G(C\hat{x} + Du) \\ \therefore \dot{\hat{x}} &= (A-GC)\hat{x} + Gy + (B-D)u\end{aligned} \quad . \tag{7}$$

We define the state error vector as follows:

$$\tilde{x} = x - \hat{x} \quad . \tag{8}$$

The state error equation is obtained and expressed as follows:

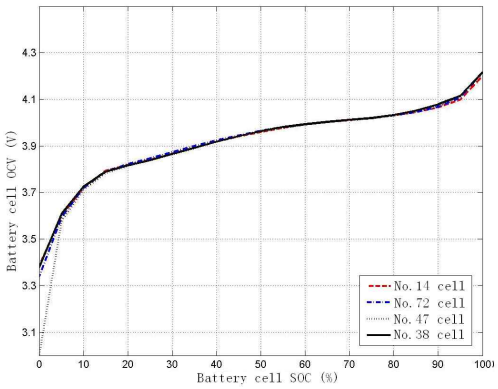

Fig. 6. Corresponding relationship between battery OCV and SOC.

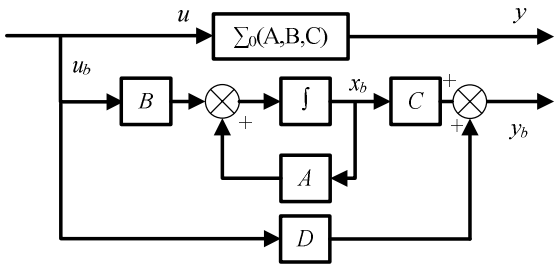

Fig. 7. Schematic of the battery state-space model.

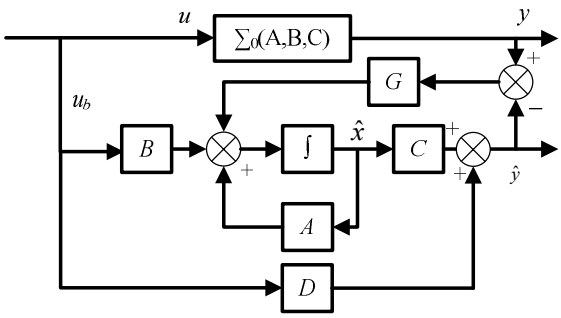

Fig. 8. Schematic of the closed-loop state observer.

$$\begin{aligned}\dot{\tilde{x}} &= \dot{x} - \dot{\hat{x}} = Ax + Bu - (A-GC)\hat{x} - Gy - Bu \\ &= Ax - (A-GC)\hat{x} - GCx \\ &= (A-GC)(x-\hat{x}) \\ \therefore \dot{\tilde{x}} &= (A-GC)\tilde{x}\end{aligned} \quad . \tag{9}$$

Eq. (9) is a homogeneous differential equation of the state error vector ($\tilde{x}$), the solution to which is as follows:

$$\tilde{x} = e^{(A-GC)t}\tilde{x}(0) \quad . \tag{10}$$

Eq. (10) shows that $\tilde{x}(0)$ is the initial value of the state error vector ($\tilde{x}$). If $\tilde{x}(0) = 0$, then state error vector $\tilde{x}$ is equal to zero, that is, the estimated state vector $\hat{x}$ is equal to the actual state for the entire period. If $\tilde{x}(0) \neq 0$, then state error vector $\tilde{x}$ approaches zero as long as all

eigenvalues of the matrix (A-GC) have negative real parts. In particular, state vector $\hat{x}$ estimated by the state observer gradually approaches the actual states. The approaching speed is dependent on the eigenvalue configuration of the matrix (A-GC). According to the principle of modern control theory, the following equation is derived as long as the battery model is observable and all eigenvalues of the matrix (A-GC) have negative real parts:

$$\lim_{t\to\infty} \tilde{x} = [x - \hat{x}] = 0 . \quad (11)$$

The theoretical analysis shows that the designed closed-loop state observer solves the problems of modeling errors, measuring errors, and random interferences by feeding back the estimation error. Moreover, it effectively solves the problem of initial battery OCV being difficult to measure in practical operations. Estimating battery SOC by using the designed state observer is theoretically feasible.

B. Designing the Gain Matrix of the Closed-Loop Observer

A key issue in designing the gain matrix of the state observer is to make the estimated battery OCV approach the actual OCV at a moderate speed. We use the pole placement method in this study. The gain matrix of the state observer is designed by analyzing the step responses of the state observer and the charging/discharging limitation of the battery in the application. Fig. 9 shows the step responses of the state observer under different pole placements. The step-responding curves when the poles of the system shift left by 0.001, 0.01, and 0.1 are illustrated in Fig. 9. Pole placement can affect the convergence speed of state U_0 (that is, U_0 denotes the equivalent OCV of the battery based on Eq. 2). When the pole is placed close to the coordinate origin, the feedback gain matrix G is small and state convergence speed is slow, and vice versa. A huge G may result in overshooting (the third curve in Fig. 9), which is an unexpected result. By contrast, a small G results in a long convergence time (the first curve in Fig. 9), which has no practical value in battery estimation. When G is set at a moderate value (the second curve in Fig. 9), overshooting does not occur and convergence speed is moderate.

V. Experimental Verification and Analysis

A practical vehicle driving test is performed to verify the designed SOC estimation method. Fig. 10 shows the test system diagram. The studied battery pack is part of the fuel cell of a hybrid vehicle power train. The battery management system and vehicle management system are connected by CAN-bus. The monitoring computer with the CAN-bus development tool CANape is used to download programs, acquire data, and calibrate control parameters. We program the estimation algorithm and embed it into the control system

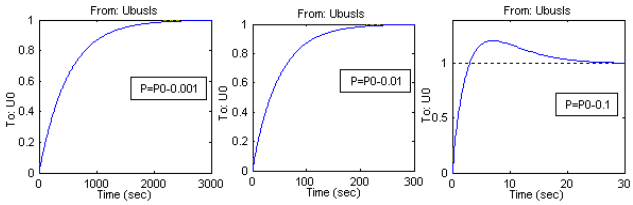

Fig. 9. Step responses of the observer under different pole placements.

TABLE I
Designed Gain Matrix of the Closed-Loop Observer under Different Pole Placements

Pole	Gain matrix
$P = P_0 - 0.001$	[0.0010 0.0010 0.0010]
$P = P_0 - 0.01$	[0.0120 0.0097 0.0082]
$P = P_0 - 0.1$	[0.3266 0.0735 −0.1002]

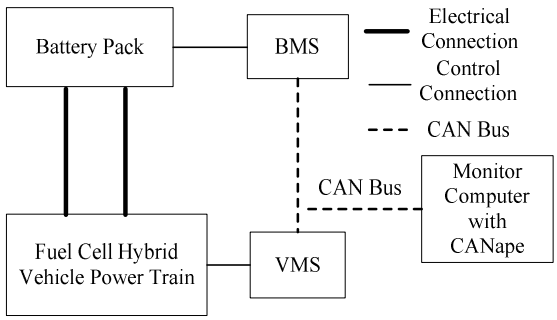

Fig. 10. Test system diagram.

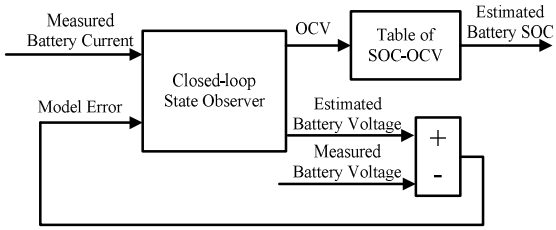

Fig. 11. Schematic of the SOC estimation program.

of the fuel cell-powered hybrid vehicle used in this study. Fig. 11 shows the schematic of the SOC estimation program. Two types of typical vehicle driving cycles test, namely, the Urban Dynamometer Driving Schedule of America (UDDS) and the Economic Commission for Europe and Extra-urban Driving Cycle (ECE-EUDC), are performed to verify and evaluate the SOC estimation method presented in this study. Fig. 12 is the window interface of the data monitoring and parameter calibration processes in the test.

Battery current and voltage data are gathered during the driving cycle test and used as input data of the SOC estimation program as shown in Figs. 13 and 14. A comparison between the SOC estimated by the state observer and the value calculated by coulomb counting under each driving cycle is illustrated in Figs. 15 and 16. Although the SOC calculated by the coulomb counting method is not

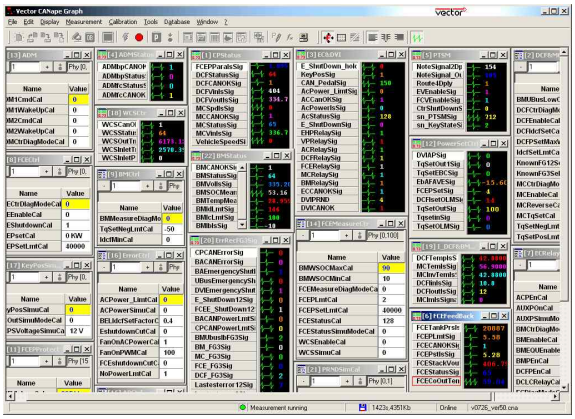

Fig. 12. Interface of data monitoring and parameter calibration processes.

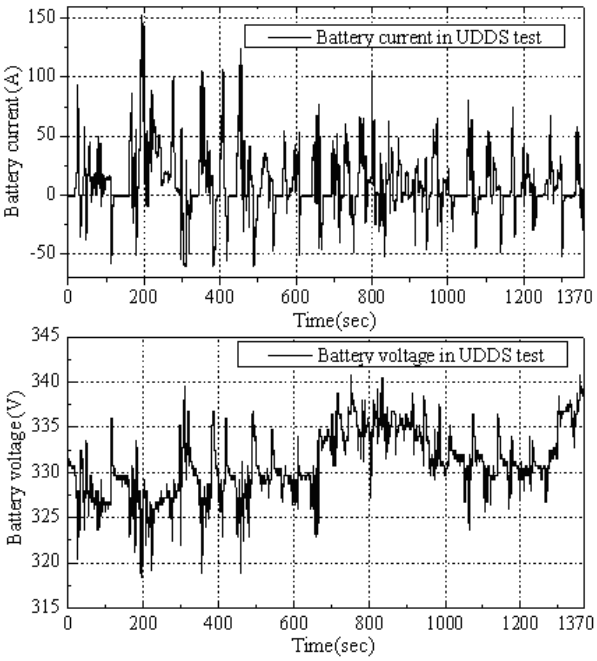

Fig. 13. Results for battery current and voltage under the UDDS test.

entirely accurate, it approximates "true" battery SOC in a relatively short time. For example, battery current is measured in this study by using a standard device with a measurement accuracy of ±0.5 A. The maximum SOC error calculated by current integration is lower than 1% in approximately 20 min. Therefore, these comparisons validate the designed SOC estimation method.

We suppose that the initial OCV of the state observer is unequal to the OCV of real battery to certify the converging speed of the estimated SOC in the experiment. This supposition is consistent with battery characteristics because the actual initial OCV can be measured in practice only if the battery is allowed to stew for approximately 3 h. To perform certification comparison, we leave the tested vehicle stewing for 3 h, measure the actual initial OCV, and consider it as the initial value of coulomb counting before each driving cycle

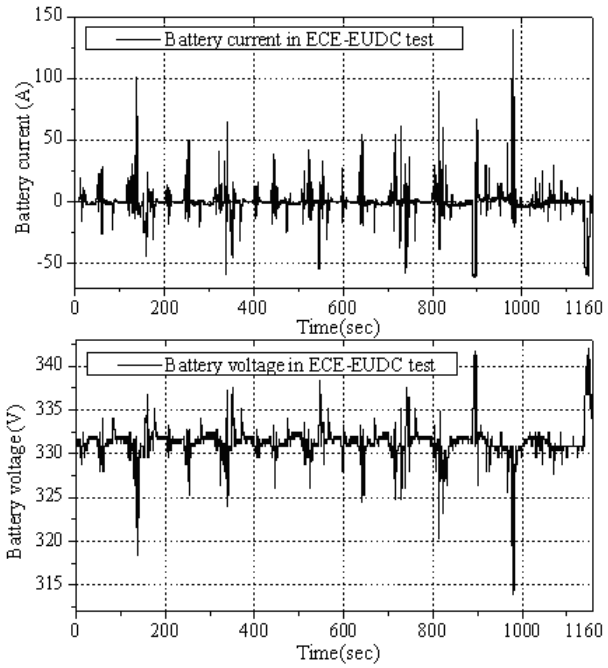

Fig. 14. Results for battery current and voltage under the ECE-EUDC test.

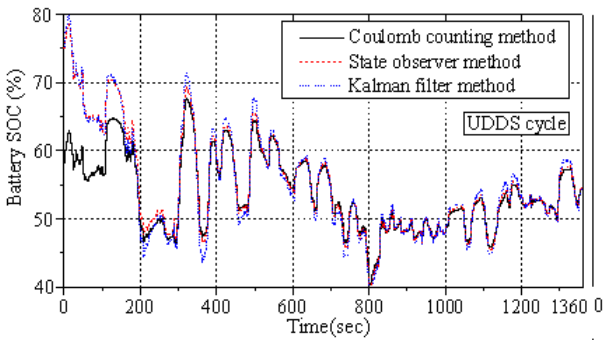

Fig. 15. Comparison among battery SOC values using the coulomb counting, state observer, and Kalman filter methods under the UDDS cycle.

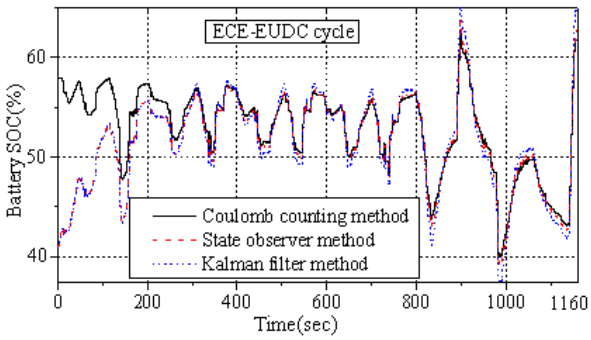

Fig. 16. Comparison among battery SOC values using the coulomb counting, state observer, and Kalman filter methods under the ECE-EUDC cycle.

test. Figs. 15 to 16 show that even if different initial OCV errors are supposed in each driving cycle test, the estimated SOC can converge rapidly to the counted SOC within approximately 200 s, which is consistent with the preceding

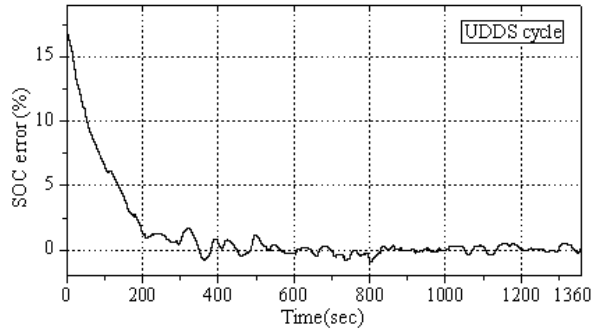

Fig. 17. Estimation error by the state observer under the UDDS cycle.

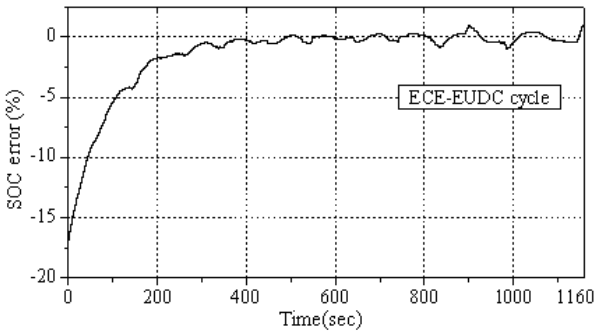

Fig. 18. Estimation error by the state observer under the ECE-EUDC cycle.

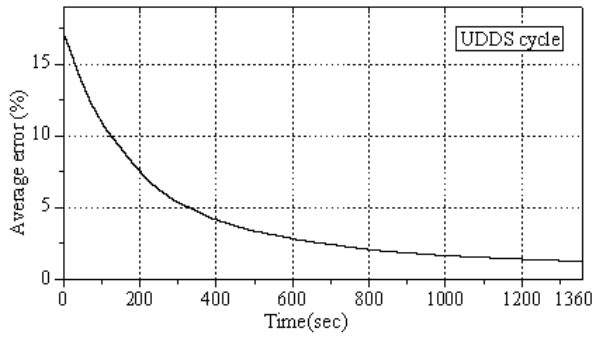

Fig. 19. Average estimation error by the state observer under the UDDS cycle.

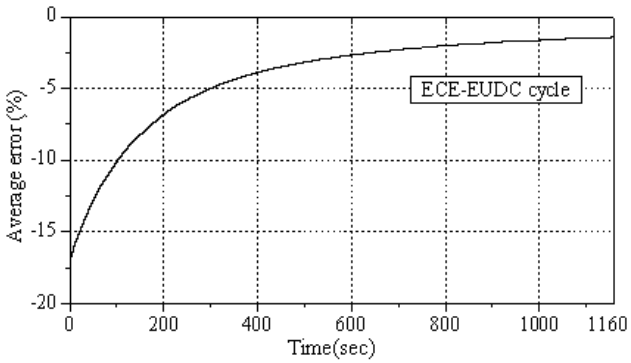

Fig. 20. Average estimation error by the state observer under the ECE-EUDC cycle.

step-response analysis (the second curve in Fig. 9). The figures also show that the proposed state observer method is better than the Kalman filter method in terms of estimation accuracy. The SOC estimation errors of the proposed estimation method under each driving cycle test are shown in Figs. 17 to 18. The average SOC estimation errors of the proposed estimation method under each driving cycle test are shown in Figs. 19 to 20. Figs. 16 to 20 show that if the supposed initial error is excluded, that is, counting from 200 s, the maximum deviation between the estimated and counted SOC values is 1.74% under the UDDS cycle and 1.77% under the ECE-EUDC cycle. Similarly, the average deviation under each driving cycle is 0.37% under the UDDS cycle and 0.43% under the ECE-EUDC cycle. In addition, we can determine from the tests that maximum deviation occurs under maximum current condition, which is consistent with the modeling error.

VI. CONCLUSIONS

1) The state-space mathematical model of lithium-ion battery is developed based on a three-order equivalent circuit model. A comparison between the results of the model simulations and the tests prove that the battery state-space model is accurate and suitable for SOC estimation.
2) A novel battery SOC estimation algorithm based on the state-space model is proposed by applying multi-state closed-loop observer theory. This method provides clear physical definitions and can be easily applied in practical control systems. Theory analyses and experiments prove that the algorithm exhibits sufficiently high accuracy for battery SOC estimation.
3) Unlike the coulomb counting SOC estimation method, the proposed SOC estimation method has two benefits. First, it effectively solves the problem of the initial battery SOC being too difficult to specify in practical applications. Second, it can eliminate the integral accumulation error via a multi-state feedback algorithm.
4) Although the proposed method does not give special consideration to the influences of system noise and measuring errors, it can reduce the influence of unmodeled factors and random interferences by feeding back deviations between the estimated and measured battery voltages.
5) Environmental temperature and battery age are factors that can gradually change the parameters of the battery model. We should take measures, such as the online model parameter estimation method, to solve such problems in a follow-up study.

ACKNOWLEDGMENT

This research is supported by the National Natural Science Foundation of China (No. 51205215), the China Postdoctoral Science Foundation (No. 2013M540488) and the Science and Technology Plan Project of Qingdao Economic and

Technological Development Zone.

REFERENCES

[1] L. Lu, X. Han, J. Li, J. Hua, and M. Ouyang, "A review on the key issues for lithium-ion battery management in electric vehicles," *Journal of Power Sources*, Vol. 226, No. 5, pp. 272-288, May 2013.

[2] X. Z. Wei, Z. C. Sun, and J. X. Tian, "Parameters identification and state estimation of lithium-ion power battery," *Journal of Tongji University*, Vol. 36, No. 2, pp. 231-235, Feb. 2008.

[3] E. Leksono, I. N. Haq, M. Iqbal, F. X. N. Soelami, and I. G. N. Merthayasa, "State of charge (SoC) estimation on LiFePO4 battery module using Coulomb counting methods with modified Peukert," in *Conf. Rec.2013 International Conference on Rural Information & Communication Technology and Electric-Vehicle Technology,* pp. 102-108, 2013.

[4] P. Singh, C. Fennie Jr., and D. Reisner, "Fuzzy logic modelling of state-of-charge and available capacity of nickel/metal hydride batteries," *Journal of Power Sources*, Vol. 136, No. 2, pp. 322-333, Oct. 2004.

[5] S. Malkhandi, "Fuzzy logic-based learning system and estimation of state-of-charge of lead-acid battery," *Engineering Applications of Artificial Intelligence*, Vol. 19, No. 5, pp. 479-485, May 2006.

[6] S. Malkhandi, "Fuzzy logic-based learning system and estimation of state-of-charge of lead-acid battery," *Engineering Applications of Artificial Intelligence*, Vol. 19, No. 5, pp. 479-485, Aug. 2006.

[7] C. Hametner and S. Jakubek, "Fuzzy observer design for local model network based battery state of charge estimation," in *Conf. Rec.2013 21st Mediterranean Conference on Control & Automation*, pp. 265-270, 2013.

[8] C. Hametner and S. Jakubek, "Design of experiments, nonlinear identification and fuzzy observer design," *Journal of Power Sources*, Vol. 238, No. 9, pp. 413-421, Sep. 2013.

[9] B. Cheng, Z. Bai, and B. Cao, "State of charge estimation based on evolutionary neural network," *Energy Convers Manage*, Vol. 49, No. 27, pp. 88–94, Nov. 2008.

[10] W.-Y. Chang, "Estimation of the state of charge for a LFP battery using a hybrid method that combines a RBF neural network, an OLS algorithm and AGA International," *Journal of Electrical Power & Energy Systems,* Vol. 53, No. 11, pp. 603-611, Nov. 2013.

[11] L. Kang, X. Zhao, and J. Ma, "A new neural network model for the state-of-charge estimation in the battery degradation process," *Applied Energy*, Vol. 121, No. 4, pp. 20-27, Apr. 2013.

[12] A. Vasebi, S. M. T. Bathaee, and M. Partovibakhsh, "Predicting state of charge of lead-acid batteries for hybrid electric vehicles by extended Kalman filter," *Energy Conversion and Management*, Vol. 49, No. 5, pp. 75-82, May 2008.

[13] H. Chao, B. D. Youn, and J. Chung, "A multiscale framework with extended Kalman filter for lithium-ion battery SOC and capacity estimation," *Applied Energy*, Vol. 92, No. 6, pp. 694-704, Jun. 2012.

[14] C. Jiang, A. Taylor, D. Chen, and K. Bai, "Extended Kalman Filter based battery state of charge(SOC) estimation for electric vehicles," in *Conf. Rec.IEEE Transportation Electrification Conference and Expo*, pp. 1-5, 2013.

[15] X. Zhou, B. Zhang, H. Zhao, W. Shen, and A, Kapoor, "State of charge estimation based on improved Li-ion battery model using extended Kalman filter," in *Conf. Rec.2013 8th IEEE Conference on Industrial Electronics and Applications*, pp. 607-612, 2013.

[16] C. Piao, M. Liu, L. Su, Z. Li, C. Cho, and S. Lu, "Study on stable estimation method for lead-acid battery SOC by extended Kalman filter," *International Journal of Control and Automation*, Vol. 7, No. 4, pp. 429-438, Apr. 2014.

[17] S. Santhanagopalan and R. E. White, "State of charge estimation using an unscented filter for high power lithium ion cells," *International Journal of Energy Resource*, Vol. 34, No. 1, pp. 152-63, Jan. 2010.

[18] J. Zhang and C. Xia, "State-of-charge estimation of valve regulated lead acid battery based on multi-state Unscented Kalman Filter," *Electrical Power and Energy Systems*, Vol. 33, No. 3, pp. 472-476, Mar. 2011.

[19] W. He, N. Williard, C. Chen, and M. Pecht, "State of charge estimation for electric vehicle batteries using unscented kalman filtering," *Microelectronics Reliability*, Vol. 53, No. 6, pp. 840-847, Jun. 2013.

[20] S. Choa, H. Jeonga, C. Hana, S. Jin, J. H. Lim, and J. Oh, "State-of-charge estimation for lithium-ion batteries under various operating conditions using an equivalent circuit model," *Computers and Chemical Engineering*, Vol. 41, No. 5, pp. 1-9, May 2012.

[21] R. Xiong, H. He, F. Sun, and K. Zhao, "Evaluation on state of charge estimation of batteries with adaptive extended Kalman filter by experiment approach," *IEEE Trans. Veh. Technol.*, Vol. 62, No. 1, pp. 108-117, Jan. 2013.

[22] S. Sepasia, R. Ghorbania, and B. Y. Liaw, "A novel on-board state-of-charge estimation method for aged Li-ion batteries based on model adaptive extended Kalman filter," *Journal of Power Sources*, Vol. 245, No. 1, pp. 337-344, Jan. 2014.

Yulan Zhao was born in Weifang, China in 1974. She received her B.S. and M.S. in Power Engineering from Shandong University of Technology, Jinan, China in 1999 and Nanjing University of Technology, Nanjing, China in 2006, respectively. She worked as an engineer at the Laiwu Power Plant from 1999 to 2003. She is currently a lecturer at the School of Automobile and Traffic, Qingdao Technological University, Qingdao, China. Her current research interests include power battery management and electric vehicles.

Haitao Yun was born in Taian, China in 1977. He received his B.S. and M.S. in Mechanical and Electronic Engineering from Shandong University, Jinan, China in 1999 and 2003, respectively. He obtained his Ph.D. in Vehicle Engineering from Tongji University, Shanghai, China in 2007. He conducted postdoctoral research in electric vehicles at Zhejiang University, Hangzhou, China from 2012 to 2013. He is currently a professor at the School of Automobile and Traffic, Qingdao Technological University, Qingdao, China. His current research interests include automotive electronics and electric vehicles.

Shude Liu was born in Zaozhuang, China in 1988. He received his B.S. in Vehicle Engineering from Shandong Jiaotong University, Jinan, China in 2003. He is currently a postgraduate student at the School of Automobile and Traffic, Qingdao Technological University, Qingdao, China.

Huirong Jiao was born in Shuozhou, China in 1990. He received his B.S. in Vehicle Engineering from Qingdao Technological University, Qingdao, China in 2003. She is currently a postgraduate student at the School of Automobile and Traffic, Qingdao Technological University, Qingdao, China.

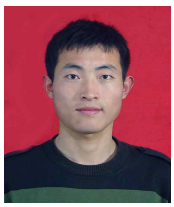

Chengzhen Wang was born in Dezhou, China in 1990. He received his B.S. in Vehicle Engineering from Qingdao Technological University, Qingdao, China in 2003. She is currently a postgraduate student at the School of Automobile and Traffic, Qingdao Technological University, Qingdao, China.